

## Article

High Temperature Magnetic Sensors<sup>†</sup>Edward Rokicki<sup>1,†</sup> , Radosław Przysowa<sup>1,†,\*</sup> , Jerzy Kotkowski<sup>1,†</sup>  and Paweł Majewski<sup>1,†</sup> <sup>1</sup> Instytut Techniczny Wojsk Lotniczych, ul. Księcia Bolesława 6, 01-494 Warsaw, Poland

\* Correspondence: radoslaw.przysowa@itwl.pl

<sup>†</sup> This paper is an extended version of our paper published in AVT-357 Research Workshop on Technologies for future distributed engine control systems (DECS) organized online by the NATO Science and Technology Organization on 11–13 May 2021.<sup>‡</sup> These authors contributed equally to this work.

**Abstract:** Magnetic sensors are widely used in health management systems for turbomachinery, but their applications in the hot zone are limited due to the loss of magnetic properties by permanent magnets with increasing temperature. The paper presents and verifies models and design solutions aimed at improving the performance of an inductive sensor for measuring the motion of rotating objects operating at elevated temperatures (200–1000°C), such as compressor and turbine blades. Physical, analog and mathematical models of the interaction of blades with the sensor were developed. A prototype of the sensor was made and its tests were carried out on the RK-4 rotor rig for the speed of 7000 rpm, in which the temperature of the sensor head was gradually increased to 1100°C. The sensor signal level was compared to that of an identical sensor operating at room temperature. The heated sensor works continuously producing the output signal whose level does not change significantly. What is more, a set of six probes passed an initial engine test in an SO-3 turbojet. It was confirmed that the proposed design of the inductive sensor is suitable for blade health monitoring of the last stages of compressors, steam turbines as well as previous generation gas turbines operating below 1000°C, even without a dedicated cooling system. In real-engine applications, sensor performance will depend on how the sensor is installed and the available heat dissipation capability

**Keywords:** high-temperature sensor; inductive sensor; blade tip timing; blade health monitoring

## 1. Introduction

The need to monitor the health of the blades of jet engines and stationary turbines results from the well-known problems with blade damage [1] caused by ingested foreign objects or material fatigue. Blade Health Monitoring (BHM) systems have good commercial prospects, especially in power generation turbines which are increasingly operated in the off-design mode due to fluctuating market demand for energy. Magnetic sensors are better suited for monitoring systems than optical [2] or capacitive sensors [3,4] because they do not require cleaning, and their signals can be processed using commonly available electronic systems. However, only sensors with high durability and reliability are acceptable.

In compressors and steam turbines, blade tip timing (BTT) systems are widely used and mature [5,6], while in gas turbines there are still significant technical challenges. This is due to the low durability and high cost of the suitable probes. What is more, a turbine disk differs significantly from a fan in terms of blade vibration measurement. It is not only higher temperature and geometry of the tip, but also the high stiffness of the blades and a different way of supporting the rotor. The deflections of the turbine blades are several dozen times smaller than the fan blades and require measurement systems with a class of higher accuracy and spatial resolution [7]. Also, the structural resonances of the casing, the axial movement of the shaft and vibrations of the turbine disk can hinder the blade vibration measurements.

BTT and tip clearance (TC) sensors have a lot in common and some types offer both measurements [8]. However, sensors can be optimized either for clearance or vibration measurement. Due to the demand for higher turbine efficiency, the industry shows more interest in high-temperature TC sensors. Capacity probes are mainly used for this purpose, but several measurement solutions based on active eddy-current principle were proposed,

e.g. [9–11]. Some interesting sensor designs in low temperature co-fired ceramics (LTCC) technology were also presented [12–14].

Permanent magnet inductive sensors known as passive eddy current sensors [15,16] do not have a high-frequency generator and detector. There is, thus, higher bandwidth and no problem with cross-talk and the carrier frequency related to the operation of the generator in active eddy-current sensors [17,18]. The disadvantage of passive sensors is the dependence of the signal on the speed, but this is much less relevant in BTT, especially in constant-speed power generation machines. Tip clearance measurement is also possible but requires dynamic calibration. Another problem is the decrease in magnetization of permanent magnets with increasing temperature. At the Curie temperature, ferromagnetic materials become paramagnetic, i.e. they completely lose their magnetic properties and are no longer a source of a magnetic field. To avoid this, the permanent magnet can be replaced in the sensor with a DC powered electromagnet [19].

Standard inductive sensors measure blade vibrations and rotational speed in machines such as compressors or steam turbines, where the sensor operating temperature does not exceed 125°C. Their high temperature versions designed for turbochargers are specified at 230°C [20,21]. However, different sensor materials and manufacturing technologies are required for high pressure compressors and gas turbines. The main difficulty in the design of high-temperature sensors is developing low-temperature sensor production technologies, which at the same time guarantee the strength of the structure at an operating temperature of 1000°C or higher. In particular, it is advisable to use materials and cements that do not need to fire the assembled sensor since this would deprive the magnets of their magnetic properties.

Most of the high temperature BTT sensors (optical and capacitive) are designed for short-term use and therefore cannot be used in BHM systems. Moreover, very few other sensors are constantly used in the engine hot section due to the high cost and the lack of materials and technologies to ensure durability. The exceptions include various types of thermometers such as optical fibres[22,23], Pt100 sensors and thermocouples, which are usually duplicated. Piezoelectric transducers such as pressure [24,25] and vibration transducers [26] have a similar problem with the Curie temperature as in inductive sensors, but there is a group of materials that work above 600°C [27,28].

Microwave sensors [7,29,30] can be made of materials that can be used up to 1400°C. Unfortunately, changes in distances in the turbine caused by thermal expansion shift the sensor's operating point, which can be compensated for by using complex electronics. Despite recent advances, microwave BTT/TC sensors have not reached full maturity yet.

The article presents selected design solutions and the results of rig testing of an inductive sensor with a permanent magnet, which can operate in gas turbines at a temperature up to 900°C. A series of measurements was made to verify the suitability of the sensor for operation in a gas turbine. In order to check the sensor's performance at elevated temperature, the head of the sensor was heated with a blowtorch from 25°C to 1100°C, comparing its signal with the response of a cold sensor aimed at the same test wheel.

## 2. Materials and Methods

### 2.1. Working Principle

The inductive tip-timing sensor is designed to measure the arrival time of blades (TOA). Like an electric generator, it uses electromagnetic induction to produce output signal as blades pass. The sensor consists of a probe and a specialized conditioning system, which can work near the turbine at a temperature as high as 150°C if it is made from high temperature electronic components [31]. The design of the probe and conditioning system must be adapted to the blade material, operating temperature and the length of the signal cable.

The field of the sensor is shaped in such a way that it reaches the blade tip. This makes the blade an integral part of the electromagnetic circuit (Figure 1). The diagram illustrates the electrodynamic interaction between the induced currents in the passing

blade  $i_1$  and the sensor winding  $i_2$ .  $R_b$  and  $X_{rb}$  are the equivalent blade resistance and leakage reactance, and  $R_s$  and  $X_s$  are the sensor resistance and reactance. A current-voltage converter produces the voltage output signal which is proportional to the sensor current  $i_2$ .

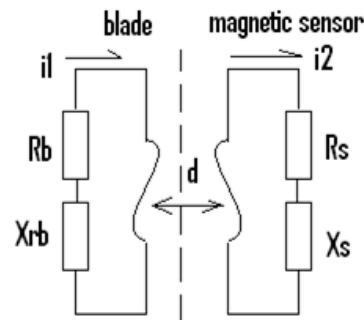


**Figure 1.** Inductive sensor circuit

The quality of the generated signal is related to the waveform parameters such as pulse amplitude, rise time and signal noise ratio [32]. The voltage reaches its maximum when the maximum energy of interaction between the blade and the sensor occurs [19]. Obtaining pulses of the appropriate quality requires the optimization of the magnetic circuit of the sensor so that the moment of force which it acts on the blade is the greatest. This is especially true if the blade is not ferromagnetic.

The range of the sensor should correspond to the variation of tip clearance during machine operation. It must not be too large especially in turbine where the blades are numerous and relatively densely spaced around the circumference. Then, the sensor interacts with two or three blades at the same time, which reduces the signal quality and resolution of the position measurement.

An earlier version of the sensor is presented in [16]. The probe design has recently been modified to improve durability, hot gas resistance and output characteristics. The solution is based on the patented high-temperature magnetic measurement technology based on the use of a pair of permanent magnets and a winding with a low number of turns [33]. The use of two magnets prevents decrease in the magnetic properties of the sensor under the effect of exhaust gases. A low-turn winding reduces the impact of temperature on coil impedance and sensor performance.

The inductive sensor (Figure 1) can detect the rotating blades made of conductive ferromagnetic or non-magnetic materials due to the wide range of gains available in the conditioning system. It can be installed in a threaded hole and fixed with an M16x1 nut. Alternatively, a bracket with a 19 mm hole and two M16x1 nuts (Figure 2) can be used.

## 2.2. Sensor Design

The probe consists of a steel body, a magnetic circuit and a heat-resistant ceramic insulator. The two-piece body is the main structural element of the sensor, designed to operate in the turbine zone under thermal stress and high vibration levels. The steel body, in order to guarantee the sensor's durability, should have proper walls of appropriate thickness, and the threads used should ensure fastening. Inside, there is an isolator, and inside the insulator - fixed elements of the magnetic circuit, i.e. two magnets and a winding.

The insulator is made of ceramics ( $\text{Al}_2\text{O}_3$  99.9% purity), fired in  $1600^\circ\text{C}$ , which can operate in high pressure and temperature existing in gas turbine. Above  $300^\circ\text{C}$ , ceramics becomes a semiconductor whose wave impedance is a function of the concentration of ions in the exhaust gas. Due to the high purity, the wave impedance of the ceramics is then about  $120\ \Omega$  (not  $1\ \Omega$  as for the contaminated one). The input impedance of the amplifier and the sensor winding is matched to the wave impedance of the hot insulator.

The ceramic insulator protrudes about 10 mm from the steel body. In this temperature range, there are no other materials than ceramics that could act as an insulator. Unfortu-

nately, if it is hit when cold, it can break easily. Due to its fragility, it should be covered as much as possible by the steel body.

The assembled sensor (Figure 3) cannot be repaired or disassembled without destroying it. The elements of the electromagnetic circuit inside the sensor cannot move. The correctness of the assembly or any damage can be checked using Computed Tomography (CT). You can also measure the winding resistance and the magnetic field of the magnets with a magnetometer.

The signal cables have glass-fiber insulation with an operating temperature of 800°C. The cables can be extended with a standard twisted pair (Ethernet cable) if needed, but this reduces the signal-to-noise ratio. The maximum possible length (typically 12 m) depends on the application: the greater the gain, the shorter the cable should be. The operation of the sensor requires a microprocessor-controlled conditioning system (Kotkowski et al. 2021), which amplifies the signal and generates a digital TTL signal.

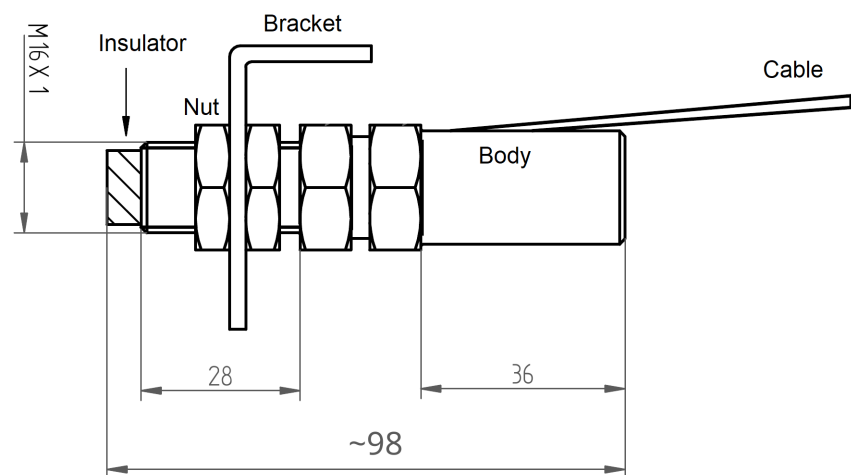


**Figure 2.** Inductive sensor



**Figure 3.** Inductive sensor - photo

### 2.3. Permanent Magnets

Strong permanent magnets (PM) are made from alloys of rare-earth elements [34,35]. Among the available types of magnets, ferrite and neodymium magnets do not work at temperatures above 200°C (Table 1). They lose a lot of their magnetic field even at a moderate temperature as high as 125°C (Fernandez et al. 2015). All magnets demagnetize when heated to the Curie temperature or a strong electromagnetic field from an AC electromagnet is applied [36].

**Table 1.** Permanent magnet properties

Property	Ferrite (HF)	AlNiCo	SmCo	NdFeB
Pull force	moderate	medium	high	very high
Curie temp. °C	450	900	750	310
Max. operating temp. °C	250	520	520	100
Corrosion resistance	very high	very high	high	low
Machining	no	diamond cutting grinding	no	no
Demagnetization with AC electromagnet	medium-resistant	not resistant	very resistant	resistant
Cost	low	high	very high	acceptable

The presented sensor uses two cooperating magnets [33]: measuring AlNiCo and supporting samarium (SmCo). The magnets are positioned on the sensor axis along which the temperature gradient occurs. The AlNiCo magnet works at a higher temperature, but is supported by the field of the larger samarium magnet. This solution makes it difficult to demagnetize the AlNiCo magnet, and the temperature is a factor that strengthens its field. Strong permanent magnetic fields and elevated temperature are used in the manufacturing of permanent magnets to improve their performance in the process known as magnetic thermal annealing or artificial magnetic ageing [37,38].

Two-magnet designs ensures that the signal parameters are maintained if the temperature of the external part of the sensor does not exceed 400°C. This can happen when the engine is shut down, when airflow ceases and the structure is not cooled. Such states in sensors with a single magnet caused their irreversible destruction. In the presented two-magnet sensor, moderate overheating stabilizes and strengthens the measurement magnet.

#### 2.4. Sensor Installation

During operation in a gas turbine, the probe comes into contact with gas at a temperature of up to 1100°C. Therefore, it should be mounted in such a way that makes heat dissipation possible so that the temperature of the external part of the sensor does not exceed 150 - 200°C during normal operation. The cooling medium may be bleed air or bypass air in a turbofan.

The sensor is installed manually in the turbine casing. It is mounted by screwing the sensor into the socket prepared in the engine nozzle to the appropriate distance from the blade. After positioning the sensor, it is fixed with a nut and connected to the configured amplifier.

Installing the sensor is the riskiest moment for its health and durability, especially for the cables and the insulator. Personnel handling sensors should be properly trained and should use the proper tools. The threads should be made so that it is not necessary to use high torques for fastening. The cables should be carefully fastened in conduits so that they are not exposed to abrasion and erosion. Fitting sensors requires removing the outer casing of the engine and usually costs much more than sensors.

#### 2.5. Sensor Durability

Turbine operators are interested in achieving the durability of the sensors for at least 5-6 years of continuous operation, which is the typical time between overhaul (TBO) of turbines, but it is difficult to simulate and prove in laboratory conditions. In steam turbines, the operating temperature is moderate (about 100°C), but the main problem is a humid environment and corrosion [39]. In case of mechanical damage to the insulator, the sensor loses its tightness and the winding and magnets corrode. In a damaged sensor, the response of the electromagnetic circuit to the blade transition decreases and gradually disappears, which is manifested by a lower signal-to-noise ratio of the output signal.

During the operation of a gas turbine, there are noticeable changes in the stand-off distance between the blades and the sensor due to rotor vibrations and thermal expansion. This is why the ceramic insulator should be flush-mounted and must not protrude into the abrasive layer. If the stand-off clearance is too small, the sensor may be rubbed and damaged [9,16].

Further work is required to predict sensor health and detect symptoms of signal deterioration. Fernandez et al. [40] tested performance of PMs subjected to cyclic magnetization and demagnetization in temperature up to 135°C. They found that magnets' cycle life decreases with operating temperature. In practice, the known methods for assessing the waveform quality are used, such as monitoring and statistical analysis of pulse amplitude, signal-to-noise ratio, rise time and the number of missing and surplus blades.

## 2.6. Rig Testing

A commercial rotor rig (Bently Nevada RK-4 Rotor Kit) was adapted to test BTT / TC sensors. A test wheel with 9 steel blades and a diameter of 120 mm was mounted on the shaft. The motor control unit was used to set the desired speed up to 10,000 rpm. The NI PXI-1065 computer equipped with PXIe-6358 module and software developed in LabView was the data acquisition system (DAQ). The block diagram of the measurement system is shown in Figure 4.

Two sensors were mounted around a test wheel. Figure 5 shows the tested sensor heated with a blowtorch on the right and the reference sensor in the bottom left corner. The temperature of the probe was measured with a thermocouple, which was attached to the ceramic insulator by means of glass silk thread, resistant to temperature up to 1060°C. The test consisted in heating the sensor until the selected temperature was reached and measuring the sensor signal for 3 minutes at a constant speed of 7000 rpm. This procedure was repeated a few times for temperature raised from 50 to 1100°C. The bladed wheel was moved away from the sensors during heating but it was moved back for spinning.

A series of measurements were made with gradually increased temperature (Figure 6). The signals from the sensors were fed into the multi-stage adjustable amplifier of the conditioning system. The amplified signals were sampled with frequency of 500 kHz. For each temperature point, 20 second of data was recorded in the pcm format and processed in Matlab.

## 2.7. Signal processing

For each temperature, the Hilbert transform  $Hx(t)$  was calculated for sensor output  $x(t)$ , for the data frame of 20 seconds. It was used to get the signal envelope  $e(t)$  as the modulus of the analytic signal:

$$e(t) = |x(t) + iHx(t)| \quad (1)$$

The average envelope voltage of the hot sensor was then related to the cold sensor's one.



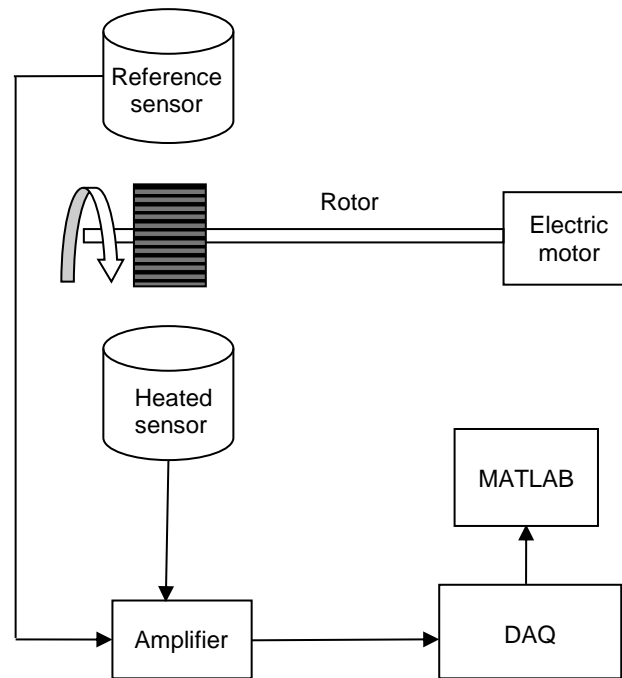


**Figure 4.** Scheme of the rotor rig and data acquisition

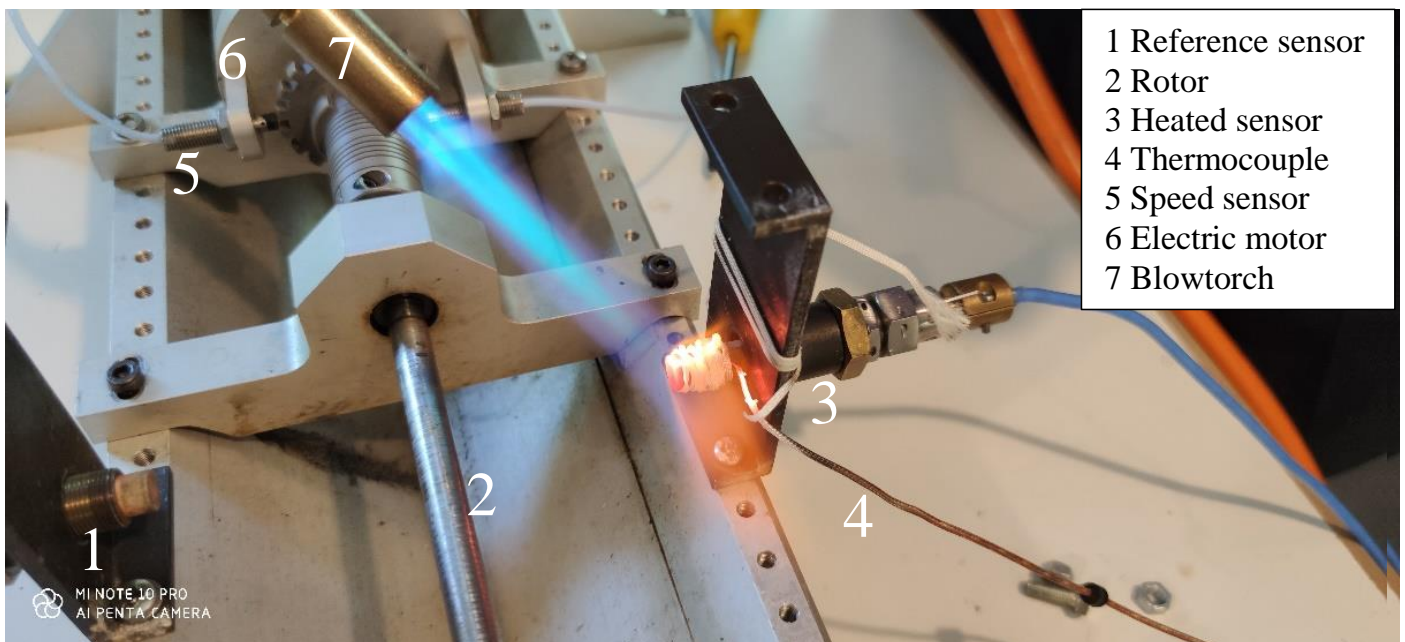


**Figure 5.** Inductive probe fired at the rotor rig

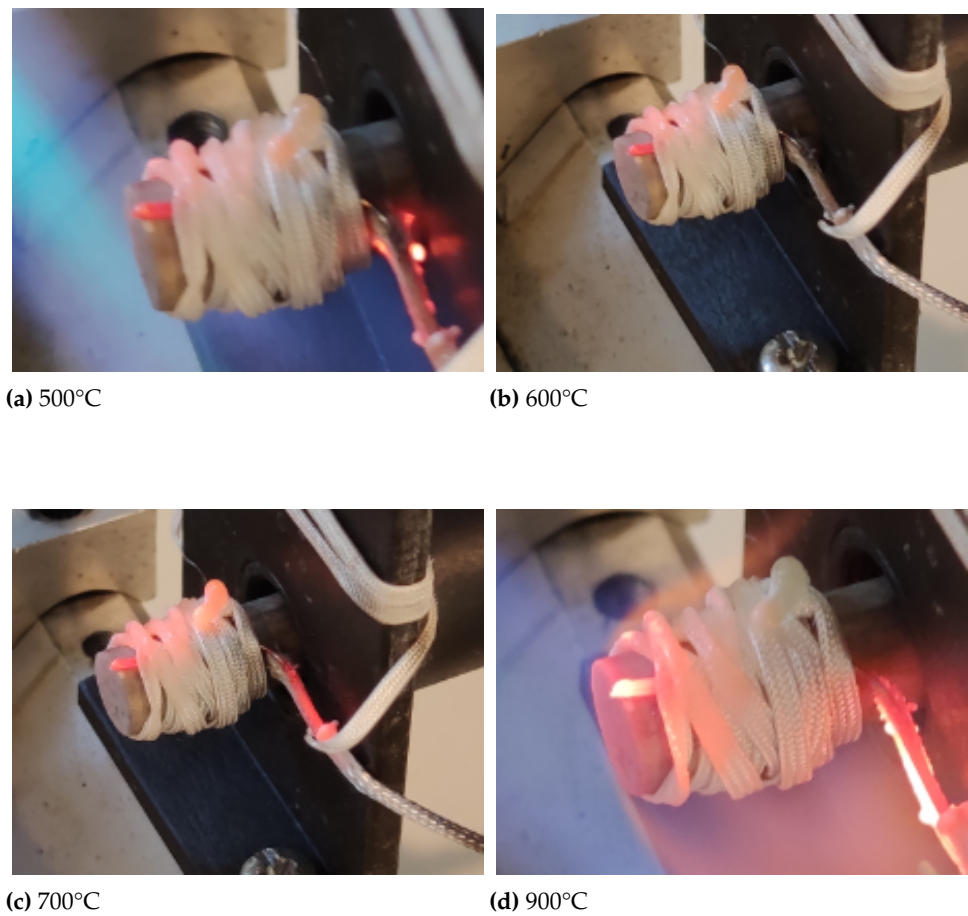


**Figure 6.** Probe at gradually increased temperature

1 **3. Results**

2 Across the whole tested temperature range (50-1100°C), both sensors generated mea-  
3 surable pulses in response to passing blades. Figure 7 and 8 show the heated probe and its  
4 output signal at 1100°C.



**Figure 7.** Probe and a thermocouple heated to 1100°C



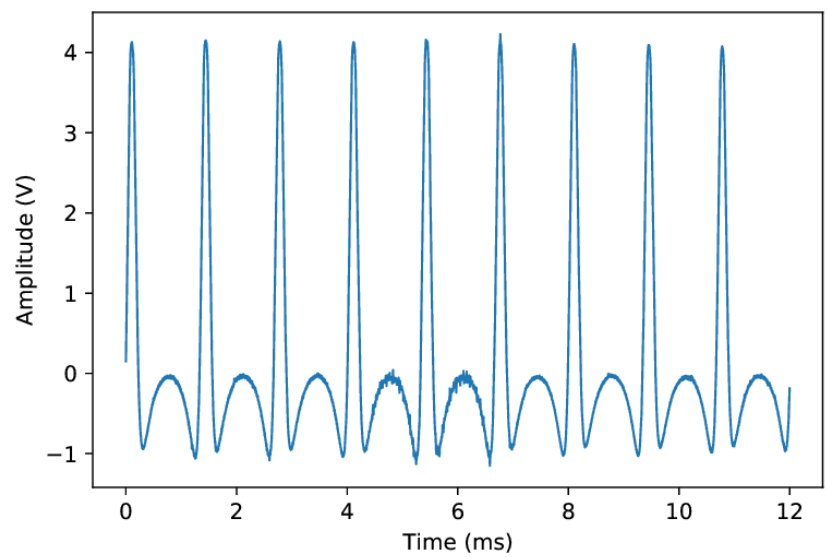


Figure 8. Output signal at 1100°C

5        The voltage level of the signal was determined for several temperatures. Figure 9  
6 shows the voltage ratio of the heated sensor signal in relation to the cold sensor. It can be  
7 seen that the sensor maintains its primary performance even at 1100°C.

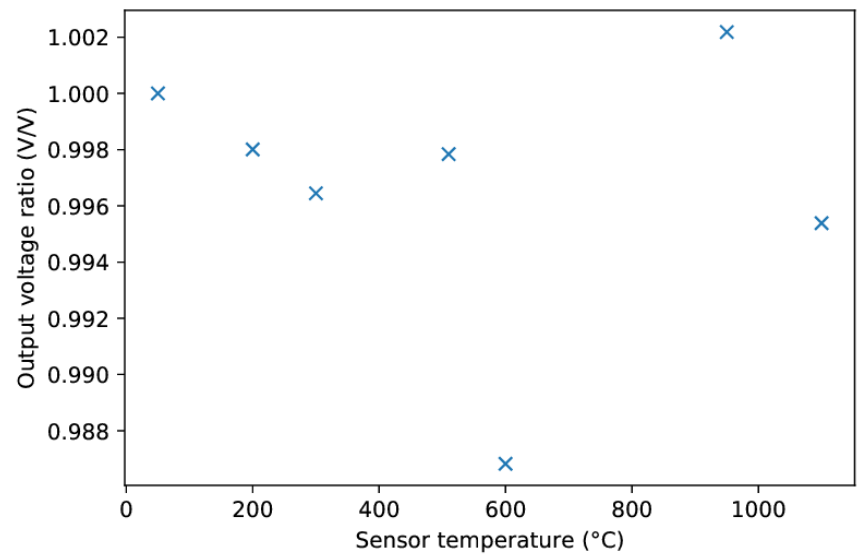
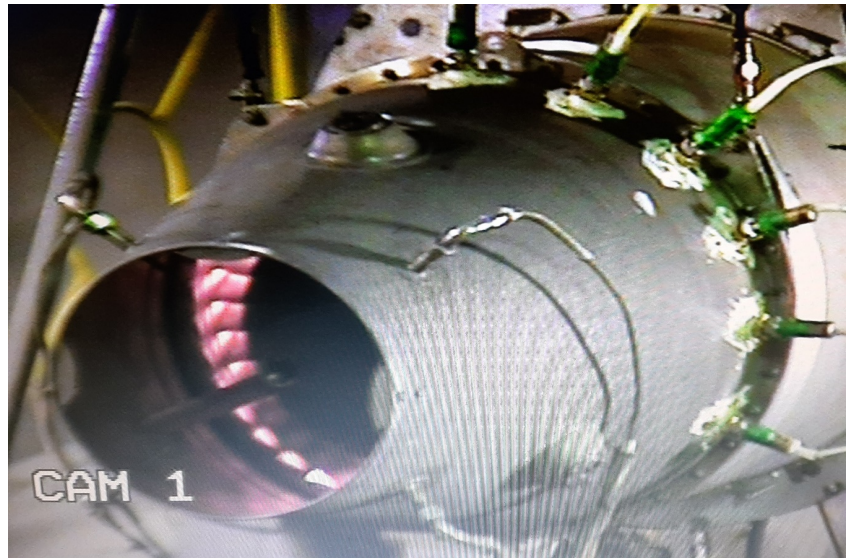
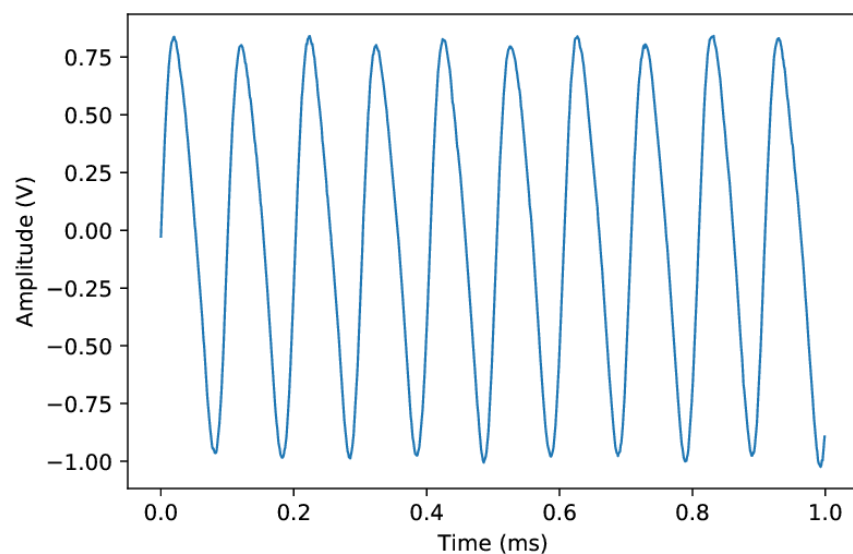


Figure 9. Hot sensor output voltage related to cold probe

8        Finally, six sensors were installed in the turbine of the SO-3 turbojet and tested (Figure  
9 10). Output signals were acquired with 1 MHz sampling. All the sensors produced readable  
10 signals for the entire test. Figure 11 and 12 show some initial data gathered at the idle (7200  
11 rpm) and takeoff speed (15600 rpm). There are 83 turbine blades, so the corresponding  
12 blade passing frequencies are 9960 Hz and 21580 Hz. The rising edge has a low rise time,  
13 so it can be used for time-of-arrival measurement.



**Figure 10.** Sensors operated in a SO-3 turbojet



**Figure 11.** Sensor 2 output for the SO-3 turbojet at idle

#### 14 4. Discussion

15 Presented rig and engine tests confirmed that hot gases had negligible influence on  
 16 the sensor output signal. Moreover, these preliminary engine tests verified the correct  
 17 operation of a set of sensors installed in the turbine casing. This provides a solid basis for  
 18 blade vibration analysis and further studies of turbine dynamics. Our prior measurements  
 19 in this turbine were performed with a single microwave sensor [7] or, later, with a previous  
 20 version of the inductive sensor [16]. There were considerable difficulties in identifying the  
 21 observed vibration responses due to the inability to conduct multi-sensor analysis.

22 The presented sensor has significant improvements in relation to its previous version.  
 23 Firstly, an insulator with much better parameters and a lower production spread was used.  
 24 It was possible thanks to the improvement of the production technology, i.e. reducing  
 25 shrinkage after firing. Low porosity and high purity and hardness of the ceramics were  
 26 achieved. These factors directly affect the durability and performance of the sensor.

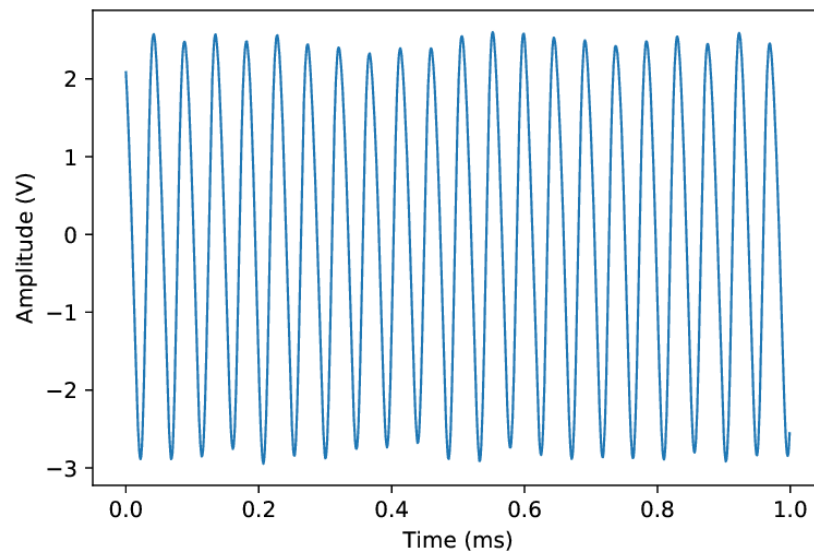


**Figure 12.** Sensor 2 output for the SO-3 turbojet at the takeoff speed

Based on operating experience with earlier versions, the geometry of the sensor and its manufacturing were optimized. In particular, the magnetic circuit of the sensor was enhanced by more efficiently matching its impedance with the input impedance of the amplifier. The implemented method of assembling the circuit and guiding the winding increased the reliability of the sensor. Thanks to the maturation of sensor's manufacturing technology, an acceptable repeatability of its parameters was achieved, which made it possible to build a multi-probe BTT system. However, sensor optimization has natural limitations related to the turbine environment, such as limited space and problems with heat dissipation.

The presented rig experiment lacked a screen simulating the turbine casing as in [9]. As a result, the sensor received more heat than in the engine, which is even better for checking its robustness. However, the measurement of temperature at only one point was a significant simplification, especially in view of the temperature gradient along the sensor needed for its correct operation. This is due to the fact that in a standard engine only the average exhaust gas temperature (EGT) is available. More thermocouples should be used in the next test or even a thermal imaging camera. It is also planned to carry out a numerical thermal analysis of the sensor. To prove the durability of the sensor, should be built a burner rig, able to perform automatic heat cycles, in which the temperature changes according to the mission profile of the aircraft engine.

Tests run on a legacy turbojet may seem not quite representative for operation of a stationary gas turbine or a commercial turbofan engine. Earlier experience with the military turbofan shows that in bypass engines it is more difficult to install and service the sensor, but there are better conditions for the natural cooling of the sensor. The use of a turbojet in the engine design is beneficial from the point of view of the cost of testing and the labor consumption of sensor assembly. However, the presented preliminary tests are insufficient to validate the reliability and durability of the sensor. Although the earlier version of the inductive sensor operated in a gas turbine for about 30 hours and at least 3 years in a steam turbine, it was possible to perform only a short engine test with this sensor design.

As for the data collected during the engine tests, we intend to carry out further analysis based on objective criteria, both in terms of waveform quality and blade vibration. In particular, the waveform parameters of the tested sensors in the different operating points will be compared. An uncertainty analysis will be carried out, which will lead to the selection of the optimal sampling rate and triggering method and determination of the

60 arrival times for all sensors. This will enable the blade vibration analysis to be performed  
61 using circumferential least squares [5,41].

62 It is expected that the acquisition system will be properly set up to generate online  
63 TOA values in planned engine tests. This will enable the characterization of turbine blade  
64 vibrations and the application of external excitation to observe responses that are normally  
65 not measurable. It is planned to equip the engine with a sensor once per revolution and an  
66 accelerometer, which will facilitate the interpretation of tip timing data.

67 Due to the physical limitations of the technology related to Curie temperature, the  
68 presented magnetic sensors with permanent magnets cannot replace capacitive or optical  
69 sensors used in the development of modern high pressure turbines. However, inductive  
70 sensors can be suitable and cost-competitive in applications where gas temperature is  
71 moderate and where there is no access to a sensor for maintenance. What is more, active  
72 cooling can significantly extend the scope of their application. The flexibility of using this  
73 type of sensor in the engine and its signal-to-noise ratio was considerably enhanced by  
74 introducing a smart conditioning unit [31], able to monitor and control the output signal  
75 level.

76 **5. Conclusions**

77 The paper presents the design and validation of a high-temperature magnetic sensor  
78 for blade health monitoring. It discusses the selection of components and technologies  
79 to build a robust and durable sensor as well as challenges related to its installation in a  
80 turbine and efforts to ensure trouble-free operation.

81 The permanent-magnet sensor was tested at a temperature of up to 1100 °C to evaluate  
82 its waveform quality and confirm the possibility of using it in the BHM systems of gas  
83 turbine blades. It was found that the signal level changes by only a percent as a result of  
84 heating. In real-engine applications, sensor performance will depend on how the sensor  
85 is installed and the available capability for heat dissipation. The proposed design of the  
86 inductive sensor is suitable for blade health monitoring of the last stages of compressors,  
87 steam turbines as well as previous generation gas turbines operating below 1000°C, even  
88 without a dedicated cooling system.

89 The presented design solutions overcome most problems related to the operation of  
90 inductive sensors in elevated temperature. They can be also implemented in other types of  
91 magnetic sensors used to measure speed or distance in the hot section of the gas turbine.  
92 The increased temperature capability of sensors and their electronics offers more flexibility  
93 in the design of the engine health management and control system which can be thus made  
94 in a distributed architecture. Robust magnetic sensors which need less wires, power and  
95 cooling are more likely to be widely implemented in future military engines.

96 **Author Contributions:** Conceptualization: E.R. and R.P.; Investigation: J.K, E.R., P.M. and R.P.;  
97 Methodology: E.R., R.P. and P.M.; Project administration: R.P.; Software: R.P. and E.R.; Supervision:  
98 R.P. and P.M.; Visualization: R.P., J.K and E.R.; Writing—original draft: R.P. and E.R.; Writing—review  
99 & editing, R.P. All authors have read and agreed to the published version of the manuscript.

100 **Funding:** This publication includes the results of the statutory activity of ITWL ‘Demonstrator of  
101 the system to measure turbine blade vibration’, financed by the Ministry of Science and Higher  
102 Education in 2018-2020.

103 **Institutional Review Board Statement:** Not applicable

104 **Data Availability Statement:**

105 **Conflicts of Interest:** The authors declare no conflict of interest.

106 **Abbreviations**

107 The following abbreviations are used in this manuscript:

108

AVT	Applied Vehicle Technology Panel
BHM	Blade Health Monitoring
BTT	Blade Tip Timing
CT	Computed tomography
DAQ	Data Acquisition system
DC	Direct current
DECS	Distributed engine control systems
100 EGT	exhaust gas temperature
ITWL	Air Force Institute of Technology in Warsaw
LTCC	Low temperature co-fired ceramics
NATO	North Atlantic Treaty Organization
RK	Rotor Kit
TC	Tip Clearance
TOA	Time of Arrival
TTL	Transistor–transistor logic

## References

1. Mevissen, F.; Meo, M. A Nonlinear Ultrasonic Modulation Method for Crack Detection in Turbine Blades. *Aerospace* **2020**, *7*, doi:10.3390/AEROSPACE7060072.
2. García, I.; Przysowa, R.; Amorebieta, J.; Zubia, J. Tip-Clearance Measurement in the First Stage of the Compressor of an Aircraft Engine. *Sensors* **2016**, *16*, 1897. doi:10.3390/s16111897.
3. Chivers, J. A Technique for the Measurement of Blade Tip Clearance in a Gas Turbine. 25th Joint Propulsion Conference; American Institute of Aeronautics and Astronautics: Reston, Virginia, 1989. doi:10.2514/6.1989-2916.
4. Fabian, T.; Prinz, F.B.; Bresseur, G.; Member, S. Capacitive Sensor for Active Tip Clearance Control in a Palm-Sized Gas Turbine Generator. *Instrumentation* **2005**, *54*, 1133–1143.
5. Przysowa, R.; Russhard, P. Non-Contact Measurement of Blade Vibration in an Axial Compressor. *Sensors* **2020**, *20*, 68. doi:10.3390/s20010068.
6. Przysowa, R. Blade Vibration Monitoring in a Low-Pressure Steam Turbine. Volume 6: Ceramics; Controls, Diagnostics, and Instrumentation; Education; Manufacturing Materials and Metallurgy; American Society of Mechanical Engineers: Oslo, 2018; pp. 1–11. doi:10.1115/GT2018-76657.
7. Szczepanik, R.; Przysowa, R.; Sychała, J.; Rokicki, E.; Kaźmierczak, K.; Majewski, P. Application of Blade-Tip Sensors to Blade-Vibration Monitoring in Gas Turbines. In *Thermal Power Plants*; Rasul, M., Ed.; InTech, 2012; pp. 145–176. doi:10.5772/29550.
8. Yu, B.; Ke, H.; Shen, E.; Zhang, T. A Review of Blade Tip Clearance–Measuring Technologies for Gas Turbine Engines. *Measurement and Control* **2020**, *53*, 339–357. doi:10.1177/0020294019877514.
9. Sridhar, V.; Chana, K.S. Tip-Clearance Measurements on an Engine High Pressure Turbine Using an Eddy Current Sensor. Volume 6: Ceramics; Controls, Diagnostics and Instrumentation; Education; Manufacturing Materials and Metallurgy. ASME, 2017, p. V006T05A014. doi:10.1115/GT2017-63803.
10. Zhao, Z.; Liu, Z.; Lyu, Y.; Gao, Y. Experimental Investigation of High Temperature-Resistant Inductive Sensor for Blade Tip Clearance Measurement. *Sensors (Switzerland)* **2019**, *19*. doi:10.3390/s19010061.
11. Borovik, S.; Sekisov, Y. Single-Coil Eddy Current Sensors and Their Application for Monitoring the Dangerous States of Gas-Turbine Engines. *Sensors* **2020**, *20*, 2107. doi:10.3390/s20072107.
12. Lai, Y. Eddy Current Displacement Sensor with LTCC Technology. PhD thesis, University of Freiburg, 2005.
13. Ihle, M.; Ziesche, S.; Gierth, P.; Tuor, A.; Tigelaar, J.; Hirsch, O. Low Temperature Co-Fired Ceramics Technology for Active Eddy Current Turbocharger Speed Sensors. *Microelectronics International* **2018**, *35*, 164–171. doi:10.1108/MI-12-2017-0067.
14. Ma, M.; Wang, Y.; Liu, F.; Zhang, F.; Liu, Z.; Li, Y. Passive Wireless LC Proximity Sensor Based on LTCC Technology. *Sensors (Switzerland)* **2019**, *19*, 1–10. doi:10.3390/s19051110.
15. von Flotow, A.; Drumm, M.J. High Temperature, through the Case, Eddy Current Blade Tip Sensors. *Sensors & Transducers Magazine (S&T e-Digest)* **2004**, *44*, 264–272.
16. Przysowa, R.; Rokicki, E. Inductive Sensors for Blade Tip-Timing in Gas Turbines. *Journal of KONBiN* **2015**, *36*, 147–164. doi:10.1515/jok-2015-0064.
17. Chana, K.S.; Sridhar, V.; Singh, D. The Use of Eddy Current Sensors for the Measurement of Rotor Blade Tip Timing: Development of a New Method Based on Integration. Volume 6: Ceramics; Controls, Diagnostics and Instrumentation; Education; Manufacturing Materials and Metallurgy **2016**, p. V006T05A019. doi:10.1115/GT2016-57368.
18. Wu, J.; Wen, B.; Zhou, Y.; Zhang, Q.; Ding, S.; Du, F.; Zhang, S. Eddy Current Sensor System for Blade Tip Clearance Measurement Based on a Speed Adjustment Model. *Sensors (Switzerland)* **2019**, *19*. doi:10.3390/s19040761.
19. Jamia, N.; Friswell, M.I.; El-Borgi, S.; Fernandes, R. Simulating Eddy Current Sensor Outputs for Blade Tip Timing. *Advances in Mechanical Engineering* **2018**, *10*, 168781401774802. doi:10.1177/1687814017748020.
20. Honeywell Introduces High Temperature Magnetic Sensors. *Sensor Review* **2000**, *20*. doi:10.1108/sr.2000.08720caf.007.



21. Jaquet turbo speed sensor for commercial and off-highway vehicles. Technical report, TE Connectivity Sensors, TE.com/sensorsolutions, 2017.
22. Murugan, M.; Walock, M.; Ghoshal, A.; Knapp, R.; Caesley, R. Embedded Temperature Sensor Evaluations for Turbomachinery Component Health Monitoring. *Energies* **2021**, *14*. doi:10.3390/en14040852.
23. Badamchi, B.; Simon, A.A.A.; Mitkova, M.; Subbaraman, H. Chalcogenide Glass-Capped Fiber-Optic Sensor for Real-Time Temperature Monitoring in Extreme Environments. *Sensors* **2021**, *21*, 1–12. doi:10.3390/s21051616.
24. Sadl, M.; Bradesko, A.; Belavic, D.; Bencan, A.; Malic, B.; Rojac, T. Construction and Functionality of a Ceramic Resonant Pressure Sensor for Operation at Elevated Temperatures. *Sensors* **2018**, *18*, 1423. doi:10.3390/s18051423.
25. Yang, J. A Harsh Environment Wireless Pressure Sensing Solution Utilizing High Temperature Electronics. *Sensors* **2013**, *13*, 2719–2734. doi:10.3390/s130302719.
26. Stevenson, T.; Martin, D.G.; Cowin, P.I.; Blumfield, A.; Bell, A.J.; Comyn, T.P.; Weaver, P.M. Piezoelectric Materials for High Temperature Transducers and Actuators. *Journal of Materials Science: Materials in Electronics* **2015**, *26*, 9256–9267. doi:10.1007/s10854-015-3629-4.
27. Turner, R.C.; Fuierer, P.A.; Newnham, R.E.; Shrout, T.R. Materials for High Temperature Acoustic and Vibration Sensors: A Review. *Applied Acoustics* **1994**, *41*, 299–324. doi:10.1016/0003-682X(94)90091-4.
28. Jiang, X.; Kim, K.; Zhang, S.; Johnson, J.; Salazar, G. High-Temperature Piezoelectric Sensing. *Sensors* **2013**, *14*, 144–169. doi:10.3390/s140100144.
29. Zhang, J.; Duan, F.; Niu, G.; Jiang, J.; Li, J. A Blade Tip Timing Method Based on a Microwave Sensor. *Sensors* **2017**, *17*, 1097. doi:10.3390/s17051097.
30. Abdul-Aziz, A.; Woike, M.R.; Anderson, R.C.; Aboumerhis, K. Propulsion Health Monitoring Assessed by Microwave Sensor Performance and Blade Tip Timing. Smart Structures and NDE for Energy Systems and Industry 4.0; Niezrecki, C.; Meyendorf, N.G.; Gath, K., Eds. SPIE, 2019, p. 25. doi:10.1117/12.2515450.
31. Rokicki, E.; Kotkowski, J.; Przysowa, R.; Filipkowski, P. Network of Smart Tip-Timing Sensors in Distributed Blade Health Monitoring System. *Preprints* **2021**, pp. 1–11. doi:10.20944/preprints202107.0026.v1.
32. Hayes, B.C. ISA-RP107.1-201x Tip Timing Waveform Quality. Technical report, International Society of Automation, 2016.
33. Rokicki, E.; Spychala, J.; Szczepanik, R.; Majewski, P. Measuring Vibrations of a Turbo-Machine Rotor Blade with the Help of an Induction Sensor in High Temperature. 8,125,215, 2012.
34. Coey, J.M. Permanent Magnet Applications. *Journal of Magnetism and Magnetic Materials* **2002**, *248*, 441–456. doi:10.1016/S0304-8853(02)00335-9.
35. Liu, S. Sm–Co High-Temperature Permanent Magnet Materials. *Chinese Physics B* **2019**, *28*, 017501. doi:10.1088/1674-1056/28/1/017501.
36. de Almeida, A.A.; Landgraf, F.J.G. Magnetic Aging, Anomalous and Hysteresis Losses. *Materials Research* **2019**, *22*, 1–6. doi:10.1590/1980-5373-mr-2018-0506.
37. Sanford, R.L. *Permanent Magnets*; US Gov. print. Office.: Washington, 1944.
38. Skomski, R.; Zhou, J.; Kirby, R.D.; Sellmyer, D.J. Magnetic Aging. Mater. Res. Soc. Symp. Proc. Materials Research Society, 2006, Vol. 887.
39. Przysowa, R.; Spychala, J.; Majewski, P.; Rokicki, E. Monitoring of Blade Vibration in a Steam Turbine Power Station. In *Dynamics of Last Stage Low Pressure Steam Turbine Rotor Blades*; Rzadkowski, R.; Szczepanik, R., Eds.; Instytut Techniczny Wojsk Lotniczych, 2017; chapter 8, pp. 183–204.
40. Fernandez, D.; Martinez, M.; Reigosa, D.; Guerrero, J.M.; Suarez, C.; Briz, F.; Alvarez, C.M.S.; Briz, F. Permanent Magnets Aging in Variable Flux Permanent Magnet Synchronous Machines. 2018 IEEE Energy Conversion Congress and Exposition (ECCE). IEEE, 2018, Vol. 56, pp. 236–241. doi:10.1109/ECCE.2018.8558075.
41. Liu, Z.; Duan, F.; Niu, G.; Ma, L.; Jiang, J.; Fu, X. An Improved Circumferential Fourier Fit (CFF) Method for Blade Tip Timing Measurements. *Applied Sciences (Switzerland)* **2020**, *10*. doi:10.3390/app10113675.